BIOCHEMISTRY
including biophysical chemistry & molecular biology

Article

pubs.acs.org/biochemistry

In Vitro Stoichiometry of Complexes between the Soluble RANK Ligand and the Monoclonal Antibody Denosumab

Kelly K. Arthur,[†] John P. Gabrielson,[†] Nessa Hawkins,[‡,⊥] Dan Anafi,[§,#] Jette Wypych,[§] Athena Nagi,[†] John K. Sullivan,[∥] and Pavel V. Bondarenko*[,§]

[†]Analytical Sciences Department, Amgen Inc., 4000 Nelson Road, Longmont, Colorado 80503, United States

[‡]Protein Sciences, Amgen Inc., One Amgen Center Drive, Thousand Oaks, California 91320, United States

[§]Process and Product Development, Amgen Inc., One Amgen Center Drive, Thousand Oaks, California 91320, United States

[∥]Inflammation Research, Amgen Inc., One Amgen Center Drive, Thousand Oaks, California 91320, United States

Supporting Information

ABSTRACT: The *in vitro* binding stoichiometry of denosumab, an IgG2 fully human monoclonal therapeutic antibody, to RANK ligand was determined by multiple complementary size separation techniques with mass measuring detectors, including two solution-based techniques (size-exclusion chromatography with static light scattering detection and sedimentation velocity analytical ultracentrifugation) and a gas-phase analysis by electrospray ionization time-of-flight mass spectrometry from aqueous nondenaturing solutions. The stoichiometry was determined under defined conditions ranging from small excess RANK ligand to large excess denosumab (up to 40:1). High concentrations of denosumab relative to RANK ligand were studied because of their physiological relevance; a large excess of denosumab is anticipated in circulation for extended periods relative to much lower concentrations of free soluble RANKL. The studies revealed that an assembly including 3 denosumab antibody molecules bound to 2 RANKL trimers (3D2R) is the most stable complex in DPBS at 37 °C. This differs from the 1:1 binding stoichiometry reported for RANKL and osteoprotegerin (OPG), a soluble homodimeric decoy receptor which binds RANKL with high affinity. Denosumab and RANKL also formed smaller assemblies including 1 denosumab and 2 RANKL trimer molecules (1D2R) under conditions of excess RANKL, 3 denosumab molecules and 1 RANKL trimer (3D1R) under conditions of excess denosumab, and larger assemblies, but these intermediate species were only present at lower temperatures (4 °C), shortly after mixing denosumab and RANKL, and converted over time to the more stable 3D2R assembly.

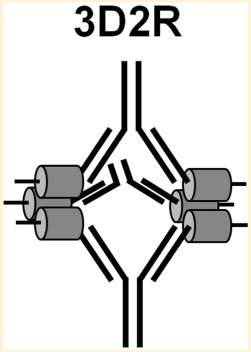

The RANK ligand (RANKL) belongs to the tumor necrosis factor (TNF) ligand family.[1,2] It binds to RANK, a receptor that mediates osteoclast formation, function, and survival. RANKL originates on the surface of osteoblast lineage cells, bone stromal cells, and other cells and binds to its receptor, RANK, on the surface of osteoclasts,[3] thereby inducing bone breakdown. Metalloproteinase cleavage of membrane-bound RANKL releases a soluble form that is fully active in stimulating osteoclast formation. Like other TNF-cytokines, cleaved RANKL has been shown to exist primarily as a trimer in solution,[4] and each RANKL trimer can bind potentially up to three receptors. Osteoprotegerin (OPG) is a soluble decoy receptor that blocks osteoclast formation by binding RANKL and preventing it from associating with RANK.[5] Denosumab is an IgG2 monoclonal antibody with specificity toward both soluble and membrane bound human RANKL. Denosumab was engineered as an IgG2 isotype, known to have little or no binding to FcγRs and, therefore, minimal immune effector functions. Previous studies have shown that denosumab binds with high affinity to RANKL (K_D = 3 pM by KinExA).[6] This binding prevents ligand association with RANK, thereby inhibiting osteoclastogenesis. To date, the binding stoichiometry of denosumab to RANKL has remained elusive. As both proteins are multivalent, it is possible that the proteins do not bind in a simple 1:1 stoichiometry, but rather combine to form more complex assemblies.

Several analytical techniques have been utilized in the field for determining binding stoichiometry and characterizing noncovalent antibody−antigen complexes, including size exclusion chromatography (SEC) in combination with static light scattering (SLS) detection,[7−12] sedimentation velocity analytical ultracentrifugation (SV-AUC),[8,11−13] and "native" electrospray ionization time-of-flight mass spectrometry (ESI TOF MS) from aqueous nondenaturing solutions.[13,14] Atomic force microscopy (AFM) is yet another technique developed for visualizing antibodies, antigens, and their complexes on a surface in a small volume of phosphate buffered saline (PBS). Solution-based techniques have an advantage in determining the stoichiometry of the noncovalent complexes compared to methods utilizing immobilization of the antibody or antigen on a surface (Biacore, KinExA, other sensor chips), which can reduce the dynamic range of the Fab arms and affect the

Received: May 20, 2011
Revised: December 23, 2011
Published: January 12, 2012

stoichiometry.[13] In this study we detail several different size separation and mass measurement methodologies to characterize the binding stoichiometry of denosumab to RANKL in physiologically relevant solutions *in vitro*.

EXPERIMENTAL PROCEDURES

Materials. Denosumab was prepared in a buffer containing sodium acetate and sorbitol. FLAG human RANK fused to human IgG1 fragment conserved (Fc) and human RANKL (containing residues 143−317) were expressed in a stable Chinese hamster ovary (CHO) cell line. RANKL was purified by anion exchange chromatography followed by cation exchange chromatography. FLAG human RANK Fc was purified using immobilized protein A. Bacterially expressed flag human RANKL (RANKL aglyco, containing residues 159−317) was purified from the soluble fraction as previously described.[2] The purified proteins were dialyzed in Dulbecco's phosphate buffered saline without calcium or magnesium (DPBS, 137 mM sodium chloride, 2.7 mM potassium chloride, 10 mM sodium phosphate, 1.76 mM potassium phosphate pH 7.4, Cellgro Cat. No. 21-031-CM). For the blended samples of denosumab and RANKL analyzed by SV-AUC and SEC, denosumab (supplied at 60 mg/mL) was added to a dilute solution of RANKL in DPBS. The order of addition was consistent across all experiments. Unless otherwise specified, the concentration of denosumab was held constant at 360 μg/mL, while the RANKL concentration was adjusted to achieve the desired molar ratio of denosumab to RANKL. Sample preparation procedures for the "native" ESI TOF MS and AFM are described below. All samples were stored at 2−8 °C and analyzed within 48 h dilution, unless indicated otherwise.

Methods. *Analytical Ultracentrifugation.* Sedimentation velocity experiments were performed using a Proteomelab XL-I analytical ultracentrifuge (Beckman Coulter) with absorbance detection at 280 nm. The exception was the analysis of low concentration samples less than or equal to 12 μg/mL where detection at 220 nm was employed. All experiments were performed in double-sector Epon centerpieces (Beckman) with quartz windows using a rotor speed of 40 000 rpm. The run temperature was controlled to 20 °C unless otherwise specified. Data analysis was performed using SEDFIT's (version 11.3) continuous $c(s)$ distribution.[15] The partial specific volumes of denosumab and RANKL were estimated to be 0.7268 and 0.7292 mL/g, respectively, from the amino acid sequence using SEDNTERP v. 1.08. As the partial specific volumes of the two proteins agree within 0.3%, when evaluating solutions containing mixtures of denosumab and RANKL, a partial specific volume of 0.7268 was applied. The solvent density and viscosity were estimated using SEDNTERP v. 1.08.

Size-Exclusion Chromatography with Static Light Scattering Detection. SEC-SLS was performed on an Agilent 1100 HPLC equipped with a variable wavelength detector (VWD). A miniDawn TriStar light scattering detector (Wyatt Technologies) was connected immediately downstream of the VWD. For both native and denaturing SEC, separation was accomplished using a flow rate of 0.5 mL/min and a Tosoh TSK guard column connected in series to two tandem Tosoh TSK Gel G3000SW$_{XL}$ columns (7.8 mm i.d. × 300 mm, 5 μm). Ambient column temperature was employed unless otherwise noted. For native SEC, 150 mM sodium phosphate, 300 mM sodium chloride, pH 7.0, was used as mobile phase. For denaturing SEC, 5 M guanidine-HCl, 0.1 M sodium phosphate, pH 6.5, was used as mobile phase. Data were collected using absorbance detection at 280 nm for both native and denaturing SEC.

The molar masses of individual peaks in the chromatograms were determined using ASTRA software (v.5.3.4.13, Wyatt Technologies). The absorptivity of denosumab at 280 nm determined from the protein sequence was 1.4 mL mg^{-1} cm^{-1}. The absorptivity of aglycosylated RANKL E-coli determined from the protein sequence was 1.76 mL mg^{-1} cm^{-1}. The absorptivity of glycosylated RANKL produced by CHO cells (taking into account that the protein is 20 wt % carbohydrate) was 1.5 mL mg^{-1} cm^{-1}. A change in refractive index with respect to concentration (dn/dc) of 0.186 mL g^{-1} was employed.[16]

Native ESI TOF Mass Spectrometry of Denosumab: RANKL Assemblies. Both glycosylated RANKL and aglycosylated RANKL E *coli* were studied. An LCT Premier TOF MS equipped with an ESI atmosphere−vacuum interface (Waters, Milford, MA) was utilized for analysis of the noncovalent complexes. Before analysis, denosumab and RANKL were buffer exchanged into 50 mM ammonium acetate aqueous solution at pH 6.8 using NAP-5 columns (GE Healthcare, Piscataway, NJ). Protein concentrations were measured by RP HPLC with UV detection at 214 and 280 nm against denosumab and RANKL standards and diluted to proper concentrations with 50 mM ammonium acetate. The "native" ESI TOF MS analysis of denosumab, RANKL and their mixtures was performed by direct infusion from a 500 μL syringe at a flow rate of 10 μL/min. The mass spectrometer was set to run in a positive ion V mode with a capillary voltage of 2600 V, sample cone 20 V, ion guide 1 at 120 V, source temperature 100 °C, desolvation temperature 400 °C, desolvation gas flow 200 L/h, cone gas flow 20 L/h, and mass range of m/z 1000−20 000. The mass spectrometer was calibrated in this range using (CsI)nCs$^+$ clusters. The calibration ESI mass spectrum of the clusters was obtained by direct infusion at 10 μL/min flow rate of CsI dissolved in 50:50 of water:acetonitrile at 20 μg/μL. This high concentration was required to generate large (CsI)nCs$^+$ clusters in the mass range up to m/z 20 000. For more efficient throughput of the large assemblies through the atmosphere−vacuum interface and transfer ion optics, ion source pressure was increased from a typical value of 1.5 Torr to 3 Torr by restricting the flow of nitrogen gas pumped out of the interface by a rough vacuum pump. For that, a valve (Speedvalve, Waters) was installed between the rough vacuum pump and the atmosphere−vacuum interface for manual restriction of the pumping flow, while the nitrogen gas flow into the ion source remained the same.

RESULTS

Size Distribution of Denosumab−RANKL Assemblies. Stock solutions of denosumab and RANKL as well as blends of the two proteins were characterized using several different size separation techniques to evaluate the binding stoichiometry of their interaction under conditions ranging from small excess RANKL in solution (1:3) to large excess denosumab (40:1). The studies were designed to examine which assembly states were possible under different concentration ratios and which were the most thermodynamically favored. SV-AUC and SEC measured size distributions for denosumab, RANKL, and four blends of denosumab−RANKL are shown in Figures 1A and 1B, respectively. SV-AUC is an important complement to SEC as it can provide superior resolution of species, and the separation by size is not limited by a column exclusion volume.

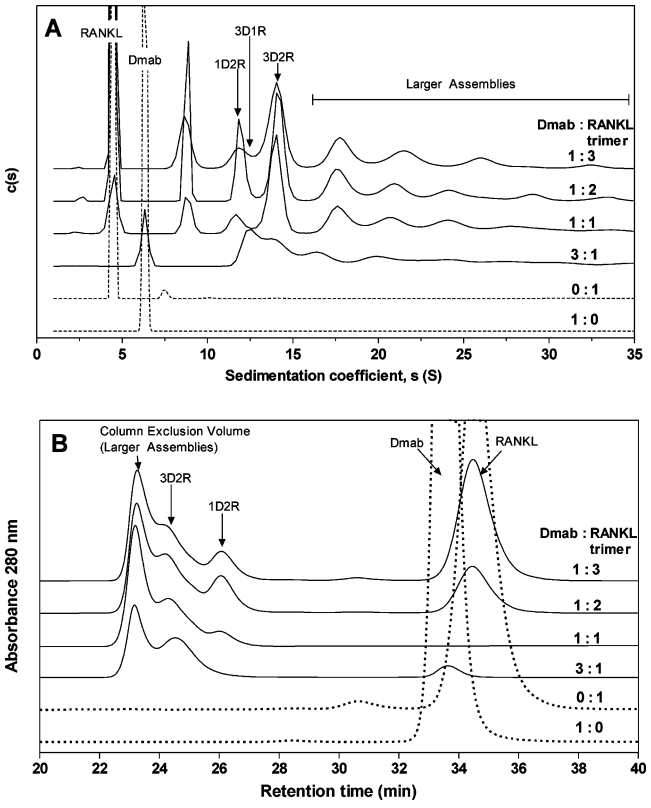

Figure 1. SV-AUC and SEC measured size distributions for denosumab (indicated by a ratio of 1:0 denosumab to RANKL), RANKL (ratio of 0:1), and four blends (3:1, 1:1, 1:2, and 1:3) of denosumab–RANKL (25× zoom). Ratios represent the molar concentration of denosumab to RANKL trimer. Unless otherwise specified, all samples were analyzed at a constant denosumab concentration of 360 μg/mL. (A) SV-AUC at 20 °C immediately after mixing; (B) SEC at ambient temperature after 24 h at 2–8 °C.

In SEC, larger species elute earlier from the column because they penetrate into the pore system of the stationary phase to a lesser extent than smaller species. Species larger than a threshold size are not separated at all and elute in the column exclusion volume (Figure 1B). Both analyses were performed using the same sample preparations. SV-AUC analysis was performed immediately after preparation while the remaining samples were held at 2–8 °C for ~24 h before SEC analysis.

The RANKL and denosumab sedimentation coefficients determined from SV-AUC analysis were 4.5 and 6.3 S, respectively (Figure 1A). For the four denosumab–RANKL blends evaluated, excess denosumab in solution was only observed for the 3:1 ratio. Excess RANKL was observed for each of the other blends by SV-AUC. Multiple species with sedimentation coefficients greater than 7 S were present for each of the blends of denosumab and RANKL (3:1, 1:1, 1:2, and 1:3, Figure 1A). These greater than 7 S species represent complexes (assemblies) of denosumab and RANKL.

Under the condition of excess denosumab (3:1 blend), assemblies with sedimentation coefficients of approximately 12.5 and 14 S along with several larger assemblies with sedimentation coefficients greater than 15 S were observed. The 12.5 and 14 S assemblies are denoted as 3D1R and 3D2R, respectively, in Figure 1A. The assembly naming specifies the number of denosumab (D) and RANKL trimer (R) molecules in each complex; the evidence for these stoichiometries will be detailed later in this section.

Under conditions of excess RANKL (1:1, 1:2, and 1:3 blends), the 14 S (3D2R) and larger assemblies were also observed, along with two additional species at approximately 8 and 11.5 S (1D2R) that were not observed under conditions of excess denosumab. The 12.5 S (3D1R) assembly was not observed when RANKL trimer was in excess.

The SEC distributions (Figure 1B) show similar trends to those observed by SV-AUC (Figure 1A), where the association of denosumab to RANKL results in the formation of multiple species. Taking into account the retention times of the species (larger assemblies elute earlier) and their peak areas, the species eluting at 26, 24.5, and 24 min by SEC (Figure 1B) correspond to the 11.5 S (1D2R), 12.5 S (3D1R), and 14 S (3D2R) assemblies detected by SV-AUC (Figure 1A). Assemblies present in the SV-AUC distributions with sedimentation coefficients greater than 14 S elute as a single peak at the SEC column exclusion volume (23 min). A peak corresponding to the 8 S SV-AUC assembly was not observed by SEC. As with SV-AUC, by SEC the 3D1R assembly was only observed under conditions of excess denosumab and the 1D2R species was only observed when RANKL was in excess. The 3D2R and larger assemblies were present regardless of which protein was in excess.

Although the SV-AUC and SEC size distributions show good agreement, some differences between the size distributions of the two methods were observed (Figure 1). Under conditions of excess RANKL a species at ~8 S was detected by SV-AUC but not observed by SEC. In addition, SV-AUC resolved multiple larger assemblies, whereas by SEC these species eluted as a single peak. Finally, no free RANKL was detected by SEC for the 1:1 blend, but some excess RANKL was observed by SV-AUC, ~10%. Differences in the distributions of species observed between SEC and SV-AUC are likely due to a confluence of factors. First, SV-AUC allows for enhanced resolution of species compared to SEC. Second, there were differences in the time between sample preparation and the time of analysis. For SV-AUC the samples were analyzed immediately after preparation versus analysis 24 h after preparation by SEC. A discussion of observed changes in the size distributions with respect to time is provided in the following section. Finally, sample dilution upon injection onto the SEC column which employed a mobile phase of 150 mM sodium phosphate, 300 mM sodium chloride, pH 7.4, could lead to dissociation of weakly associated species.

Stability and Equilibration of Complexes and Stoichiometry When Denosumab Is in Large Excess. Additional studies were performed to evaluate the stability of the denosumab–RANKL assemblies. Specifically, the effects of temperature, time after mixing, concentration, and excess reagent (denosumab or RANKL) were evaluated. The first three conditions were evaluated by SV-AUC due to the method's enhanced resolution of the denosumab–RANKL assemblies, while the effect of excess reagent was evaluated by SV-AUC and SEC.

To confirm assemblies observed at 20 °C (Figure 1A) are representative of those present at physiological temperature, three preparations of denosumab–RANKL containing excess RANKL (1:1, 1:2, and 1:3) and 4 preparations containing excess denosumab (40:1, 20:1, 10:1, and 3:1) were evaluated by SV-AUC experiments at 37 °C immediately after preparation (Figure 2A). For each preparation evaluated, the levels of larger assemblies present were lower at 37 °C compared to 20 °C. The sedimentation coefficients of the species observed in

dx.doi.org/10.1021/bi2007806 | *Biochemistry* 2012, 51, 795–806

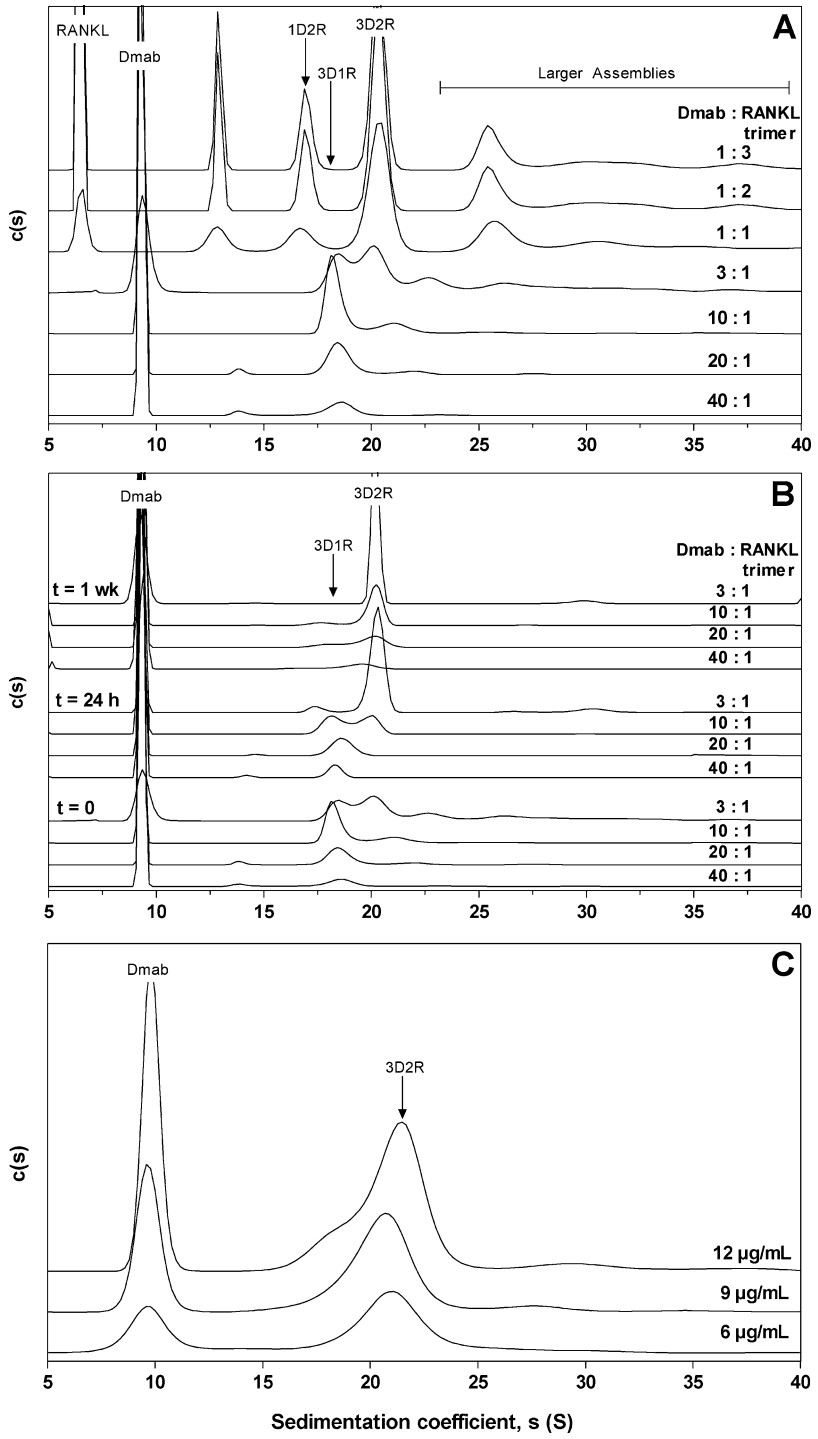

Figure 2. SV-AUC measured size distributions for denosumab–RANKL blends analyzed at physiological temperature, 37 °C. Ratios represent the molar concentration of denosumab to RANKL trimer. Unless otherwise specified, all samples were analyzed at a constant denosumab concentration of 360 μg/mL. (A) SV-AUC of preparations containing excess RANKL (1:1, 1:2, and 1:3) and excess denosumab (3:1, 10:1, 20:1, and 40:1) analyzed immediately after mixing; (B) SV-AUC of preparations containing excess denosumab analyzed immediately after mixing, after 24 h at 37 °C, and after 1 week at 37 °C; and (C) SV-AUC of 3:1 preparations at denosumab concentrations of 6, 9, and 12 μg/mL. Samples were held for 6 h at 37 °C prior to analysis.

Figure 2A were shifted to higher values compared to Figure 1A due to differences in solution viscosity at 37 °C compared to 20 °C, which results in differences in the rate of sedimentation. By conversion of the assembly sedimentation coefficients in Figures 1A and 2A to $s_{20,w}$ (experimental sedimentation coefficients converted to the conditions of water at 20 °C), it was confirmed that the species at approximately 17, 18, and 20 S in Figure 2A correspond to assemblies 1D2R, 3D1R, and 3D2R, respectively (data not shown).

Results from the excess RANKL preparations (1:1, 1:2, and 1:3) analyzed at 37 °C were in agreement with the results at 20 °C. The assemblies observed at 20 °C, the 8 S assembly (12.5 S at 37 °C), 1D2R, and 3D2R, were also present at 37 °C. For all three preparations of excess RANKL the dominant assembly

dx.doi.org/10.1021/bi2007806 | *Biochemistry* 2012, 51, 795–806

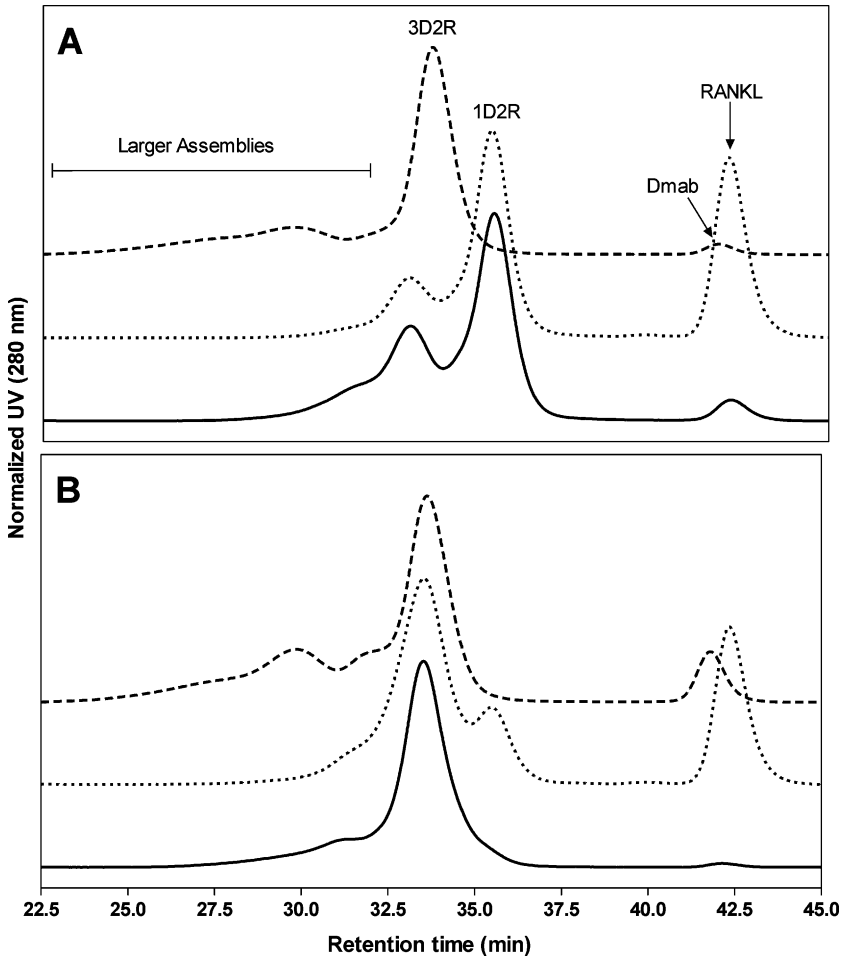

Figure 3. SEC analysis of purified fractions of the (A) 1D2R assembly and (B) 3D2R assembly collected into solutions of DPBS (solid line), DPBS with RANKL (dotted line), or DPBS with denosumab (dashed line). Chromatograms were normalized to the maximum signal intensity.

was 3D2R. When denosumab was present in large excess (40:1, 20:1, 10:1), assembly 3D1R, with a sedimentation coefficient between that of assembly 1D2R and assembly 3D2R, at ~18 S, was the predominant assembly immediately after mixing (Figure 2A). The profile of the 3:1 preparation analyzed at 37 °C (Figure 2A) was in agreement with the observations at 20 °C (Figure 1A). For the 3:1 preparation under both temperature conditions, assemblies 3D1R and 3D2R were present in similar amounts immediately after mixing. Some assembly 3D2R was also present for the 10:1 preparation in Figure 2A; however, the dominant assembly was assembly 3D1R. Little to no assembly 3D2R was observed for the 20:1 and 40:1 preparations immediately after mixing (Figure 2A).

The effect of time on the denosumab–RANKL assemblies was evaluated for the four preparations containing excess denosumab (40:1, 20:1, 10:1, and 3:1 denosumab to RANKL trimer). Each sample was evaluated at three time points: immediately after preparation, after 24 h incubation at 37 °C, and after 1 week incubation at 37 °C (Figure 2B). Because of the long run times of SV-AUC analysis, typically 6 h, short time intervals were not possible. After 24 h incubation at 37 °C, a decrease in assembly 3D1R and a corresponding increase in assembly 3D2R were observed for the 3:1 and 10:1 preparations. For all preparations, after 1 week at 37 °C, assembly 3D1R was shown to dissociate and assembly 3D2R was the dominant assembly. The three excess RANKL preparations (1:1, 1:2, and 1:3, Figure 2A) at time zero were also analyzed after 24 h incubation at 37 °C (data not shown) and showed only a slight change in their size distributions. For all excess RANKL preparations, assembly 3D2R persisted as the dominant assembly and the relative amounts of larger assemblies and assembly 1D2R declined slightly. The results suggest that regardless of which molecule is initially present in excess, when given adequate time the equilibrium distribution shifts toward the formation of assembly 3D2R.

The 3:1 blends of denosumab and RANKL shown earlier (Figures 1 and 2A,B) to form predominantly assembly 3D2R, used an arbitrary high concentration of denosumab (360 μg/mL). To extend these studies and examine denosumab concentrations (6, 9, and 12 μg/mL) that are observed *in vivo*,[18] additional SV-AUC experiments at physiological temperature were performed. Blends of 3:1 denosumab to RANKL were prepared by dilution into DPBS equilibrated to 37 °C. Samples were held for 6 h at 37 °C prior to analysis. Data acquisition was performed at 37 °C with detection at 220 nm. The SV-AUC size distributions revealed (Figure 2C) that at low concentrations of denosumab assembly 3D2R remained dominant. Assemblies 1D2R and 3D1R were either not observed or in such low abundance that they were not well resolved from assembly 3D2R. The larger assemblies above 20 S accounted for less than 6% of the total absorbance.

To evaluate the stability of assembly 1D2R and assembly 3D2R in the presence of small excess denosumab or RANKL, purified SEC fractions of 1D2R and 3D2R were collected into

dx.doi.org/10.1021/bi2007806 | *Biochemistry* 2012, 51, 795–806

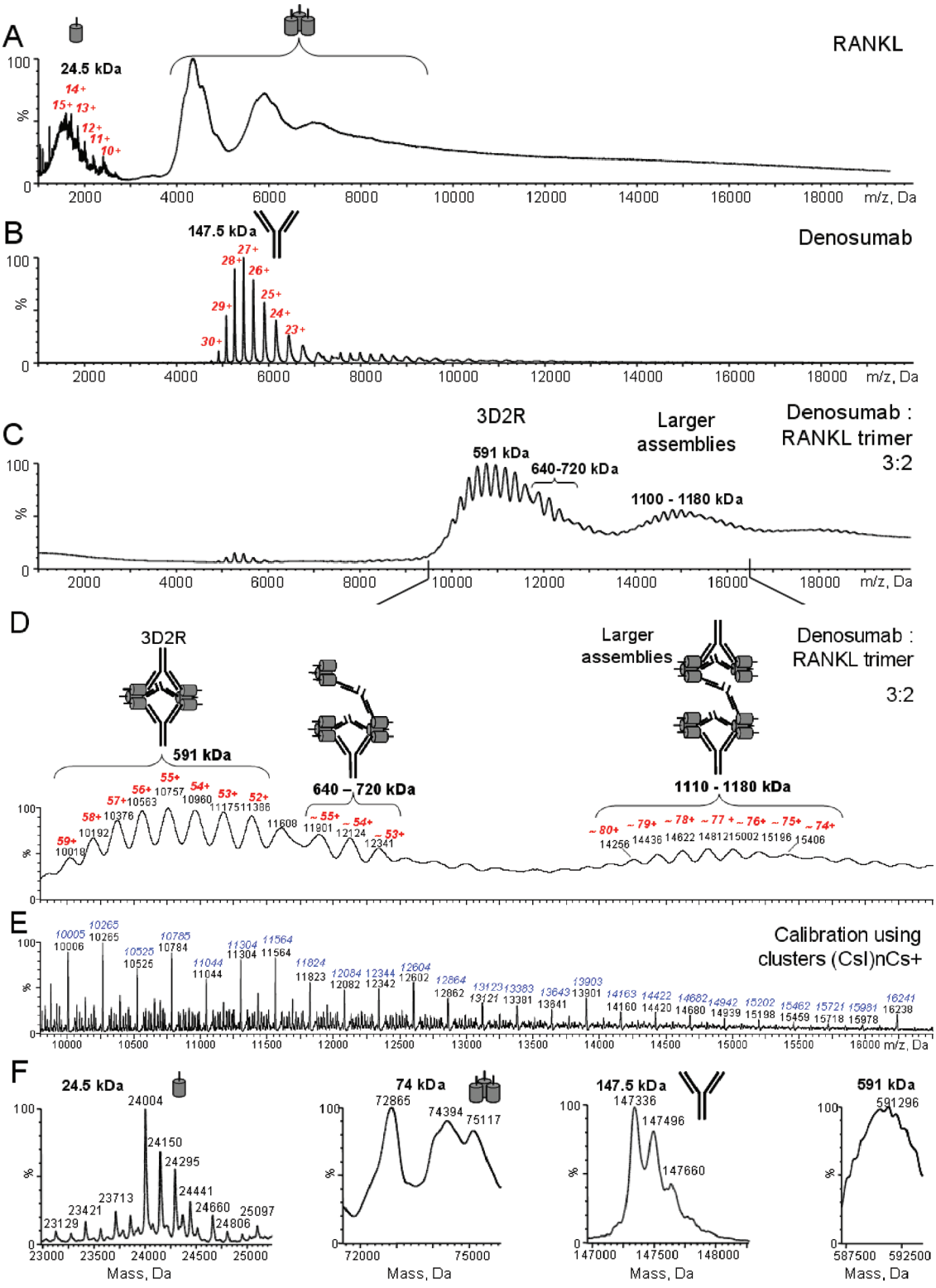

Figure 4. Electrospray ionization mass spectra of (A) RANKL at 0.08 μg/μL, (B) denosumab at 0.2 μg/μL, and (C) their mixture at molar ratio of 3:2 of denosumab:RANKL trimer and concentrations of 0.1 and 0.04 μg/μL, respectively, in 50 mM ammonium acetate. (D) Magnified view of the dominant assembly 3D2R and larger assembly region from (C). (E) Calibration mass spectrum of $(CsI)nCs^+$ clusters with measured masses in black and theoretical masses in blue and italics. (F) Deconvoluted ESI mass spectra of the multiply changed ions created by RANKL, denosumab, and their assemblies.

each of the following solutions: DPBS, DPBS containing RANKL and DPBS containing denosumab. After collection, each solution was immediately reanalyzed by SEC (Figure 3). All experiments were carried out at ambient temperature. Assembly 1D2R appeared stable when collected into DPBS and RANKL (Figure 3A). However, when collected into a solution containing denosumab, all of assembly 1D2R was converted to assembly 3D2R and larger assemblies. On the basis of the

dx.doi.org/10.1021/bi2007806 | *Biochemistry* 2012, 51, 795–806

results of the temperature dependence studies, these larger assemblies would likely dissociate at physiological temperature. This result suggests that assembly 1D2R becomes a building block for assembly 3D2R after addition of denosumab.

When assembly 3D2R was collected into DPBS, denosumab, and RANKL-containing solutions, only small changes to the size distribution were observed (Figure 3B). When the 3D2R assembly was collected in the presence of excess denosumab, some larger assemblies were formed, but assembly 3D2R remained the dominant species. Again, the species larger than assembly 3D2R would likely dissociate at physiological temperature based on the results shown in Figure 2. When assembly 3D2R was collected in the presence of excess RANKL, some assembly 1D2R was formed, but this accounts for only 13% of the total size distribution. These results support the conclusion that assembly 3D2R is the thermodynamically favored binding stoichiometry of denosumab to RANKL.

Measurement of Masses of Denosumab−RANKL Assemblies by Native ESI TOF Mass Spectrometry. The high resolution and mass accuracy of the ESI TOF MS enabled accurate measurement of the masses in the gas phase. Both glycosylated RANKL produced in mammalian cells (Figure 4) and aglycosylated RANKL produced in *E. coli* (Supporting Information Figure S1) were utilized for this analysis. Mass analyzers, including the TOF mass analyzer used in this study, measure mass indirectly as mass-to-charge ratio (m/z) as shown in Figures 4A−E. The electrosprayed proteins appear in the positive ESI mass spectra as multiple peaks on the m/z scale, each with a different number of charges (z) due to the different number of protons acquired from the electrospray solution.[19] Denosumab produces several clearly resolved peaks in the range of m/z 5000−6000 with the number of charges from 30+ to 23+. Molecular weight (m) of a protein can be calculated from any peak by multiplying its m/z value by the number of charges (z). Although multiplicity of the peaks complicates ESI mass spectra of large proteins, it improves mass accuracy and precision by providing multiple measurement of the molecular weight. The charges can be assigned to the peaks either manually using a relatively simple algorithm[19] or automatically using a deconvolution software program, like MassLynx program from Waters used in this study. The deconvoluted ESI mass spectra, generated by the deconvolution software program (Figure 4F), show molecular weight values of proteins. A deconvoluted ESI mass spectrum of denosumab shows several peaks near 147.5 kDa. They are 162 Da apart due to the variation in the number of terminal galactose residues on two biantennary oligosaccharides typically observed on human IgG2 antibodies. More abundant glycosylation of proteins broadens the mass peaks, reduces ionization efficiency, and complicates the deconvolution. Broad peaks and relatively small numbers of peaks in ESI mass spectra decrease accuracy of charge assignment and mass determination. The glycosylated RANKL produced broad poorly resolved peaks above m/z 4000 due to the variable number of sugar antennas and sialic acid residues on RANKL trimers and possibly other oligomers (Figure 4A). The ESI mass spectrum of RANKL also contained a series of better defined peaks below m/z 2000 (Figure 4A). The deconvoluted mass spectrum of these peaks produced multiple mass peaks of the glycosylation profile from 23 to 26 kDa with an average mass of 24.5 kDa of RANKL monomer (Figure 4F). The observation of RANKL monomers and dimers (Figure 1A and Figure S1) was unexpected because these species were not observed during SEC and SV-AUC analyses described above. RANKL monomers and dimers were observed in the ESI mass spectra from the 50 mM ammonium acetate solution, suggesting that a small part of RANKL trimers may be disrupted by the electrospray ionization conditions or by the 50 mM ammonium acetate solution conditions with relatively low ionic strength. Therefore, these additional species are likely artifacts of the method due to the limited stability of trimeric RANKL during ESI or in ammonium acetate, which may cause unfolding and subunit dissociation. In the deconvoluted mass spectrum of monomeric RANKL (Figure 4F), two series of peaks 292 Da apart were detected, which is a mass of sialic acid residue and a typical sign of glycosylation. The difference between the measured mass of 24.5 kDa and calculated mass of the protein portion of the RANKL monomer of 19.7 kDa indicated that ∼20% of RANKL mass was due to the glycosylation. These heterogeneous oligosaccharides broadened the mass peaks (to 23−25 kDa, Figure 4F), hence decreasing the accuracy of mass measurements. The glycosylated RANKL trimer (and possibly other oligomers) produced even broader and poorer resolved peaks above m/z 4000 (Figure 4A). The deconvolution procedure using MassLynx software revealed several broad peaks near 74 kDa (Figure 4F), which matched the expected mass of the RANKL trimer. Of particular note, the mass spectrum of denosumab mixed with RANKL trimer was dominated by relatively sharp peaks in the range of m/z 9500−11 500 (Figure 4C,D) with a deconvoluted mass of 591 kDa (Figure 4F), which is consistent with a complex composed of 3 denosumab antibody molecules bound to 2 RANKL trimers (3D2R). In addition to this predominant assembly, two other species were detected with masses of 640−720 and 1100−1180 kDa. The masses of these species were consistent with an intermediate complex and a dimer of the main complex, respectively (Figure 4C,D). There was no free denosumab or RANKL remaining in the ESI mass spectra for denosumab:RANKL blended at 3:2 ratio (3D2R, Figure 4C,D), further suggesting that this is the binding stoichiometry. The assembly state of 3 denosumab antibodies and 2 soluble RANKL trimers represents the minimum number of molecules necessary to satisfy the valencies of a bivalent antibody bound to a trivalent ligand. When either denosumab or RANKL was in excess in the blends, the peaks due to free denosumab or RANKL, respectively, would appear in the ESI mass spectra below m/z 10 000 in Figure 4C (data not shown). The mass measurements by ESI-TOF MS were performed at room temperature within ∼1 h after the buffer exchange to 50 mM ammonium acetate and blending of denosumab and RANKL. On the basis of the SV-AUC results, it is likely that the additional, less abundant and larger assemblies are transitional assemblies present prior to complete equilibration of the sample. It is also possible that these additional species may be artifacts of the method due to the poor stability of trimeric RANKL during ESI or in ammonium acetate, which may cause unfolding and subunit dissociation. To improve mass accuracy measurements for RANKL, the same experiment was repeated with aglycosylated RANKL and yielded very similar results (Figure S1 and related text). Apart from the unexpected subunit dissociation, the predominant gas-phase complex of denosumab:RANKL trimer at a 3:2 ratio reflects the main interaction state of these molecules in solution.

Determination of Stoichiometries of the Predominant Denosumab−RANKL Assemblies in Solution by SEC-SLS Followed by Denaturing SEC. To determine the size of the assemblies in solution as well as the ratio of the constituents,

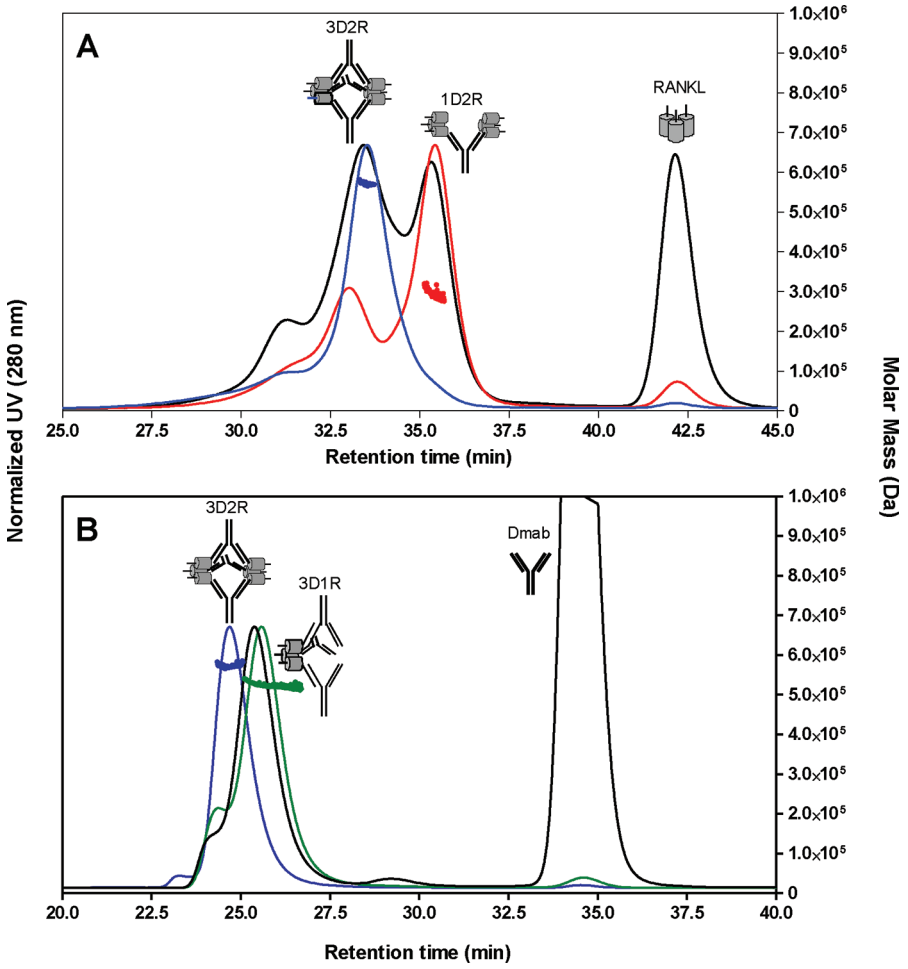

Figure 5. Size exclusion chromatograms with UV and static light scattering (SLS) detection of purified fractions of (A) 1D2R (red line) and 3D2R (blue line) assemblies overlaid with denosumab−RANKL stock preparation containing excess RANKL (black line) and (B) the 3D1R (green line) and 3D2R (blue line) assemblies overlaid with denosumab−RANKL stock preparation containing excess denosumab (black line). The molar mass measured by SLS for each fraction is plotted as closed circles. (Different column settings were used in (A) and (B), resulting in different elution time.) Chromatograms were normalized to the maximum absorbance signal intensity of the predominant denosumab−RANKL assembly.

the denosumab−RANKL assemblies 1D2R, 3D1R, and 3D2R were assessed by SEC with SLS detection under native conditions and by SEC under conditions to denature and dissociate the assemblies. Evaluation of the 8 S assembly observed by SV-AUC (Figure 1) was not possible as it was not observed by SEC. Purified fractions of the assemblies were collected after elution from the SEC column. Assemblies 1D2R and 3D2R were collected from a denosumab−RANKL preparation containing excess RANKL, while assembly 3D1R was collected from an excess denosumab preparation. Separation conditions utilized for assembly 1D2R and 3D2R fraction collection differed slightly from the conditions used in Figure 1B. Briefly, two tandem Tosoh TSK Gel G4000 columns were employed for separation followed by fraction collection in order to achieve improved resolution of species. Separation conditions for assembly 3D1R were identical to those used in Figure 1B.

To enrich for assemblies 1D2R and 3D2R (and to reduce the presence of larger assemblies), excess RANKL preparations of denosumab−RANKL were incubated overnight at 37 °C. Immediately following two rounds of purification, each fraction was reanalyzed by SEC-SLS to assess peak purity and assembly molar mass. An overlay of the size exclusion chromatograms for stock material and purified fractions is shown in Figure 5A. The purity of the assembly 3D2R enriched fraction was 97%. The purity of the assembly 1D2R enriched fraction, however, was only 48% even though a narrow time window and multiple rounds of purification were used for sample collection. This result was not unexpected based on the results of the assembly stability study (Figure 3), which revealed that the 1D2R assembly converted to 3D2R assemblies and released free RANKL upon conversion. The SEC-SLS weight-averaged molecular weight of purified assembly 1D2R was found to be ∼296 kDa. The molecular weight of purified assembly 3D2R was found to be ∼576 kDa (Figure 5A). Within the error of the measurement of ∼7% (this value refers to the precision of the measurement based on internal qualification of the method), the SLS measured molecular weight of assembly 3D2R is consistent with the molecular weight of the predominant denosumab−RANKL assembly of 591 kDa measured in gas phase by ESI TOF MS.

To enrich for assembly 3D1R, fractions were collected from a stock denosumab−RANKL preparation containing excess denosumab prepared the day of collection. An overlay of the chromatograms for stock material and purified assembly 3D2R is shown in Figure 5B. As a reference, a purified fraction of assembly 3D2R using the same column set up is also displayed in Figure 5B (blue line). The purity of assembly 3D1R was

dx.doi.org/10.1021/bi2007806 | *Biochemistry* 2012, 51, 795−806

Table 1. Molar Composition of Denosumab and RANKL Trimer in Purified Assemblies 1D2R, 3D2R, and 3D1R[a]

		dSEC peak area (mAU s)		dSEC peak mass (μg)		moles	
assembly	SEC-SLS molecular mass (kDa)	Dmab	RANKL	Dmab	RANKL	Dmab	RANKL
1D2R	296	3091.2	2915.3	18.4	16.2	1	1.70
3D2R	576	4822.2	1622.2	28.7	9	3	1.82
3D1R	535	71700.4	14009.6	426.8	77.8	3	1.06

[a]To derive the moles of denosumab and RANKL trimer present in each assembly, the peak mass of each molecule (denosumab or RANKL trimer) measured by denaturing SEC was divided by the SEC-SLS determined molecular mass of native denosumab (147 kDa) or RANKL trimer (76 kDa), respectively. The resulting moles of denosumab and RANKL trimer were multiplied by a constant factor to adjust the moles of denosumab to a whole number.

86%, and the SEC-SLS molecular weight of the purified assembly was 535 kDa. The SEC-SLS results were consistent with the SV-AUC findings, which suggest the size of assembly 3D1R, based on the sedimentation coefficient, is somewhere between assembly 1D2R and assembly 3D2R.

The purified fractions were then separated under denaturing SEC conditions to dissociate the assemblies and determine the relative concentration of denosumab and RANKL in each fraction. The peak areas and relative fractions of denosumab and RANKL determined from denaturing SEC are listed in Table 1. The chromatograms from denaturing SEC for denosumab, RANKL, and assemblies 1D2R, 3D1R, and 3D2R are shown in Figure S2. Assembly 1D2R, which is present only under conditions of excess RANKL, was found to be 50% denosumab and 50% RANKL by mass, which is consistent with a single molecule of denosumab bound to two RANKL trimers (1D2R), based on the known molecular weight values of denosumab and RANKL (147 and 76 kDa, respectively, by SEC-SLS). Assembly 3D2R, present in all mixtures, was found to be 75% denosumab and 25% RANKL by mass, in agreement with three denosumab molecules bound to two RANKL trimers (3D2R). Finally, assembly 3D1R, which is present only under conditions of excess denosumab in solution, was found to be approximately 85% denosumab and 15% RANKL by mass, which is consistent with 3 denosumab molecules bound to one RANKL trimer (3D1R).

AFM of Denosumab, RANKL, and Their Mixture. AFM images of denosumab:RANKL trimer mixed at 1:1 molar ratio (Figure S3) revealed species which, according to their sizes, correspond to assembly 3D2R and larger assemblies also detected by SEC, SV-AUC, and native ESI TOF MS. Similar to the data shown in Figures 1 and 4, AFM images in Figure S3 were acquired at ambient temperature shortly after blending the stock solutions of denosumab and RANKL, which can explain the observation of larger assemblies present with assembly 3D2R. These larger assemblies are not observed after incubation for >24 h at physiological temperatures according to the SV-AUC and SEC studies.

Interaction of Denosumab–RANKL Assemblies with RANK. Previous studies utilizing Biacore and other surface-based methods have indicated that denosumab binds RANKL with very high affinity.[6] In order to investigate if the engagement of RANKL in the assemblies with denosumab blocks it from binding to RANK, we evaluated binding by SEC (Figure 6). Denosumab and RANKL were mixed together to form the complexes, and then RANK-Fc was added at 1:1 ratio with respect to denosumab. The experiment showed that the presence of RANK did not have an effect on the denosumab–RANKL assemblies when RANKL trimer was at the same molar concentration as denosumab or at a molar concentration lower than denosumab. However, when the relative molar

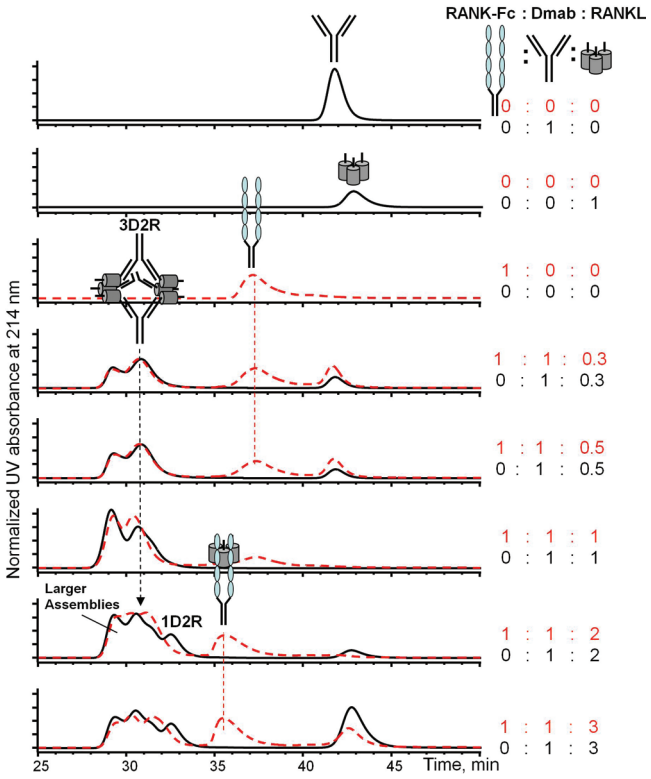

Figure 6. Size exclusion chromatograms of denosumab:RANKL mixtures (solid traces) and denosumab:RANKL:RANK-Fc mixtures (dashed traces). Denosumab and RANKL were mixed together at different ratios, and then RANK-Fc was added at 1:1 ratio with respect to denosumab. After 30 min incubation in PBS at room temperature the mixtures were placed in an autosampler at 4 °C for SEC analysis. The conditions of SEC separation were similar to those described in Figure 3, but two columns of a smaller diameter of 4.6 mm and a lower flow rate of 0.15 mL/min were utilized.

abundance of RANKL trimer exceeded denosumab, the excess RANKL trimer formed complexes with RANK, as expected (Figure 6, bottom, red dashed trace). In addition to the RANK–RANKL trimer complex eluting at 36 min, a minor peak increased at 31.5 min. This peak was not present in the chromatograms when only RANK and RANKL were mixed (data not shown), suggesting that all three molecules—RANK, RANKL, and denosumab—may be involved in the species eluting at 31.5 min. This species appears to develop only in relative molar excess of RANKL and RANK with respect to denosumab. In summary, denosumab–RANKL assemblies did not bind to RANK according to the employed SEC binding assay with the exception of significant excess of RANKL and RANK.

dx.doi.org/10.1021/bi2007806 | Biochemistry 2012, 51, 795–806

DISCUSSION

Interactions between RANKL and denosumab, a fully human monoclonal anti-RANKL antibody, were assessed in this study. Previously, free soluble RANKL (usually detected with Biomedica Gruppe ELISA kit using OPG capture) was measured in human plasma at 1−10 pg/mL level (0.2−0.6 pM;[20] 0.08 pM (1.6 pg/mL),[21] 0.69 pM[22]). Total circulating concentration of soluble RANKL, including OPG-bound plus free RANKL, was measured using Apotech ELISA kit at approximately 0.1 μg/mL.[22] A typical denosumab dose of 60−120 mg (0.9−1.7 mg/kg human) produced serum concentrations of denosumab of approximately 5−10 μg/mL,[18] which is significantly higher than total RANKL and orders of magnitude higher than free RANKL concentrations. As with most protein therapeutics and their targets, it is difficult to ascertain their relative concentrations at various sites of action in disease states for which they are indicated. RANKL, which can exist in soluble and membrane-bound forms, is likely to be found at lower concentrations in peripheral blood than in target tissues or diseased tissues including bone marrow and inflamed joints. The current work therefore explored a range of molar concentration ratios for denosumab and RANKL to identify possible binding interactions and their relative thermodynamic stability. The commonly used methodologies to study protein−protein interactions, e.g. Biacore and KinExA, require immobilization of one of the proteins of interest. This immobilization reduces the range of motion of the Fab arms of IgG antibodies and for multivalent proteins can inhibit access to binding sites, preventing the determination of the true binding stoichiometry in solution.[13] In this study several orthogonal size separation methodologies, (SV-AUC, SEC, AFM, and native ESI-TOF mass spectrometry) were applied to determine the binding stoichiometry of denosumab to RANKL. All of these methods allowed for analysis of the binding interactions in solution and in gas phase without protein immobilization. The studies described in this article revealed the predominant denosumab−RANKL assembly consisted of 3 denosumab molecules bound to 2 RANKL trimers (Figure 7, 3D2R). The formation of this complex, and the concomitant dissociation of all other complexes with incubation at 37 °C, is likely a thermodynamically driven process as less energetically favorable species relax to the dominant assembly state at equilibrium. The 3D2R species is energetically favored because it is composed of the minimum number of molecules required for all binding sites on both proteins to be occupied. Interestingly, osteoprotegerin (OPG), a homodimeric receptor which also binds with high affinity to RANKL, has been shown to prefer a 1:1 binding stoichiometry with RANKL trimer.[5] An important distinction is that OPG−Fc dimer, utilized in the study in ref 5, is envisioned to have both OPG TNFR domains deeply inserted into 2 of 3 grooves of the RANKL trimer. In contrast, only one of the two denosumab antigen binding regions (Fabs) interacts with a single trimer, allowing the second Fab to interact with a separate trimer.

Several transition intermediate denosumab−RANKL assemblies were observed (1D2R, 3D1R, and larger assemblies). A 1D1R assembly was also observed but only by SV-AUC. The species at 8 S (Figure 1A) is smaller than the 1D2R assembly, it is formed only under conditions of excess RANKL, and it is not present in RANKL alone. These observations suggest that the 8 S species in Figure 1A is 1D1R. Several other species from the proposed reaction scheme (Figure 7) were not detected by the

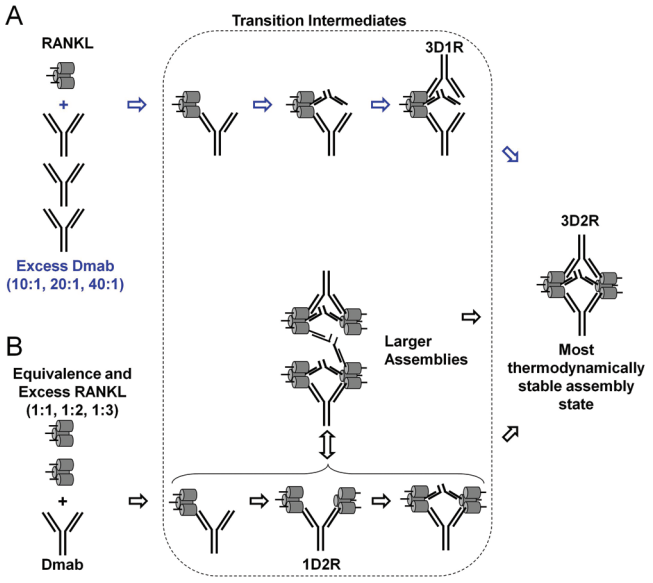

Figure 7. Proposed reaction schemes of denosumab and RANKL interactions and formation of their complexes. (A) When denosumab is present in molar excess, the reaction pathway proceeds through the assembly of an intermediate complex of 3 denosumab molecules bound to 1 RANKL trimer (3D1R). (B) When RANKL is present in molar equivalency or excess, a precursor complex consisting of 1 denosumab and 2 RANKL trimers (1D2R) is formed. Only the labeled assemblies were captured and their stoichiometry was determined. In both schemes, the reaction ultimately favors formation of assembly 3D2R.

utilized techniques, including complexes of 2 molecules of denosumab and 1 RANKL trimer and 2 molecules of denosumab and 2 RANKL trimers. We expect that these assemblies exist in our experiments, but only as short-lived precursors to assemblies 1D2R, 3D1R, and 3D2R, and remain undetectable on the time scale of our measurements (Figure 7). In these studies, we determined the most favorable binding stoichiometry under defined *in vitro* conditions, but it is important to note that *in vivo* the levels of RANKL can vary depending on the tissue, and denosumab concentrations will vary over time following dosing.[18]

Denosumab binding (J.K.S., unpublished) has been localized to the DE loop region of human RANKL,[2] a polar region (tip) of the cylindrically shaped elongated RANKL molecule that is opposite from the RANKL-expressing cell surface. (Note that in our schematics of soluble RANKL the remnant of the stalk region that attaches the ligand to the cell surface is depicted by a short rod.) The relatively small propeller-like complexes are possible because binding of two Fab arms of a denosumab antibody to the tips of two different RANKL trimers, facing each other, does not create steric hindrance at the center of the complex. This is different from the binding stoichiometry reported for the 5c8 antibody to soluble CD40 ligand (CD40L) trimer.[23] That antibody bound to equatorial (middle) regions of soluble CD40L trimers to form large, snowflake-like complexes.[23] The small, propeller-like complexes were not possible because 5c8 antibodies could not cross-link two CD40L trimers facing each other. It is important to note that the 5c8 antibody also formed large, snowflake-like aggregates on Jurkat cells expressing membrane-bound CD40L.[23] This is because the 5c8 antibody could cross-link separate ligand trimers that are side-by-side and facing the same direction,

dx.doi.org/10.1021/bi2007806 | *Biochemistry* 2012, 51, 795−806

which was a possible arrangement on the cell surface. The 5c8 antibodies disappeared from the cell surface after 2 h, most likely due to internalization.[23] Denosumab, however, binds polar sites of two RANKL ligand trimers facing each other, which is only possible in solution and not likely to occur on the cell surface. Thus, on cells, denosumab is not likely to form large complexes with RANKL as is observed with the 5c8 antibody which binds to an equatorial site of CD40L. Irrespective, denosumab binds both forms of RANKL, soluble and membrane-bound (unpublished), to block receptor recognition.

The results of our studies on the interaction of denosumab and soluble RANKL are consistent with the reaction scheme and complexes illustrated in Figure 7. When RANKL is present in excess, a single denosumab antibody molecule binds one then two RANKL trimers to form assembly 1D2R (an intermediate form), and then other denosumab molecules bind the remaining free binding epitopes of the RANKL trimers to create assembly 3D2R (Figure 7B). When denosumab is present in excess over soluble RANKL, three denosumab molecules bind to a single RANKL trimer (3D1R), wherein each antibody is associated with one subunit (Figure 7A). Given sufficient time, the assemblies re-equilibrate to form the more stable 3:2 assembly (3D2R). Under the time scale of a biological assay (5 days[6]) and the life of denosumab in circulation (from weeks to months[18]), all intermediate assemblies would be converted to 3D2R assembly, which blocks RANKL from interactions with RANK according to the *in vitro* SEC binding assay (Figure 6). When denosumab is present is excess (as it would occur *in vivo* after dosing), 3D1R and then 3D2R complexes are formed, wherein all subunits of the RANKL trimer are in a complex with an antibody "arm" (Figure 7A), and osteoclast formation is fully suppressed.[6]

The following observations suggest that assembly 3D2R (3 denosumab molecules bound to 2 RANKL trimers) is the most stable denosumab−RANKL complex. Purified assembly 1D2R converted to produce a significant amount of assembly 3D2R and free RANKL trimer. When denosumab was added to assembly 1D2R, it was entirely converted to assembly 3D2R, and a small amount of larger species. This indicates that assembly 1D2R is a relatively weak complex or a building block for the other assemblies. The larger assemblies were abundant only at lower temperatures (4 °C and room temperature) and immediately after the mixing of denosumab and RANKL. They were observed during experiments in which the blended solutions were kept at low temperatures, SV-AUC, SEC (Figures 1 and 6), and AFM (Figure S4), but were present only at trace levels when incubated at 37 °C (Figure 2) and, therefore, may not be physiologically relevant. These observations suggest that the larger assemblies form during the mixing from the assemblies 1D2R and 3D2R and cross-linking antibodies or RANKL molecules. With time and at physiological temperature, the larger assemblies dissociate to form the more stable assembly 3D2R. Denosumab is a fully human monoclonal antibody specific to RANKL that inhibits osteoclast formation, activation, and survival. Using multiple complementary size separation techniques, we show here for the first time that the most stable complex of denosumab with soluble RANKL is an assembly containing three antibody molecules bound to two RANKL trimers.

■ ASSOCIATED CONTENT

Supporting Information

Figure S1: electrospray ionization mass spectra of aglycosylated RANKL, denosumab, and their mixture at molar ratio of 3:2 of denosumab:RANKL trimer; Figure S2: size exclusion chromatograms under denaturing conditions of the assemblies 1D2R, 3D2R, and 3D1R; Figure S3: atomic force microscopy images of (A) denosumab, (B) RANKL, and (C) denosumab:RANKL trimer at 1:1 molar ratio; likely interpretations of the assemblies on the images were provided on the basis of sizes of the species. This material is available free of charge via the Internet at http://pubs.acs.org.

■ AUTHOR INFORMATION

Corresponding Author

*Phone: 805-447-7215. Fax: 805-447-3259. E-mail: pavel.bondarenko@amgen.com.

Present Addresses

[⊥]Neurozon LLC, 1884 Eastman Avenue, Ste 101, Ventura, CA [#]91320.

[#]Oncobiologics, 7 Clarke Drive, Cranbury, NJ 08512.

■ ACKNOWLEDGMENTS

We thank Paul Kostenuik, Mike Treuheit, Thomas Dillon, Zhulun Wang, Nigel Walker, Paul Schnier, Margaret Karow, Brent Kendrick, Mehul Patel, Joseph Phillips, David Brems, and Jim Thomas for fruitful discussions.

■ ABBREVIATIONS

RANKL, RANK ligand; Dmab, denosumab; TNF, tumor necrosis factor; OPG, osteoprotegerin; DPBS, Dulbecco's phosphate buffered saline; SEC, size exclusion chromatography; SLS, static light scattering; SV-AUC, sedimentation velocity analytical ultracentrifugation; ESI TOF MS, electrospray ionization time-of-flight mass spectrometry; AFM, atomic force microscopy; D, denosumab; R, RANK ligand; 3D2R, 3 denosumab and 2 RANKL molecules.

■ REFERENCES

(1) Wong, B. R., Rho, J., Arron, J., Robinson, E., Orlinick, J., Chao, M., Kalachikov, S., Cayani, E., Bartlett, F. S. III, Frankel, W. N., Lee, S. Y., and Choi, Y. (1997) TRANCE is a novel ligand of the tumor necrosis factor receptor family that activates c-Jun N-terminal kinase in T cells. *J. Biol. Chem. 272*, 25190−25194.

(2) Lacey, D. L., Timms, E., Tan, H. L., Kelley, M. J., Dunstan, C. R., Burgess, T., Elliott, R., Colombero, A., Elliott, G., Scully, S., Hsu, H., Sullivan, J., Hawkins, N., Davy, E., Capparelli, C., Eli, A., Qian, Y. X., Kaufman, S., Sarosi, I., Shalhoub, V., Senaldi, G., Guo, J., Delaney, J., and Boyle, W. J. (1998) Osteoprotegerin ligand is a cytokine that regulates osteoclast differentiation and activation. *Cell 93*, 165−176.

(3) Martin, T. J. (2004) Paracrine regulation of osteoclast formation and activity: milestones in discovery. *J. Musculoskelet. Neuronal. Interact. 4*, 243−253.

(4) Ito, S., Wakabayashi, K., Ubukata, O., Hayashi, S., Okada, F., and Hata, T. (2002) Crystal structure of the extracellular domain of mouse RANK ligand at 2.2-A resolution. *J. Biol. Chem. 277*, 6631−6636.

(5) Schneeweis, L. A., Willard, D., and Milla, M. E. (2005) Functional dissection of osteoprotegerin and its interaction with receptor activator of NF-kappaB ligand. *J. Biol. Chem. 280*, 41155−41164.

(6) Kostenuik, P. J., Nguyen, H. Q., McCabe, J., Warmington, K. S., Kurahara, C., Sun, N., Chen, C., Li, L., Cattley, R. C., Van, G., Scully, S., Elliott, R., Grisanti, M., Morony, S., Tan, H. L., Asuncion, F., Li, X., Ominsky, M. S., Stolina, M., Dwyer, D., Dougall, W. C., Hawkins, N., Boyle, W. J., Simonet, W. S., and Sullivan, J. K. (2009) Denosumab, a

fully human monoclonal antibody to RANKL, inhibits bone resorption and increases BMD in knock-in mice that express chimeric (murine/human) RANKL. *J. Bone Miner. Res. 24*, 182−195.
(7) Sanny, C. G. (2002) Antibody-antigen binding study using size-exclusion liquid chromatography. *J. Chromatogr., B: Anal. Technol. Biomed. Life Sci. 768*, 75−80.
(8) Qian, R. L., Mhatre, R., and Krull, I. S. (1997) Characterization of antigen-antibody complexes by size-exclusion chromatography coupled with low-angle light-scattering photometry and viscometry. *J. Chromatogr., A 787*, 101−109.
(9) Santora, L. C., Kaymakcalan, Z., Sakorafas, P., Krull, I. S., and Grant, K. (2001) Characterization of noncovalent complexes of recombinant human monoclonal antibody and antigen using cation exchange, size exclusion chromatography, and BIAcore. *Anal. Biochem. 299*, 119−129.
(10) Rehder, D. S., Chelius, D., McAuley, A., Dillon, T. M., Xiao, G., Crouse-Zeineddini, J., Vardanyan, L., Perico, N., Mukku, V., Brems, D. N., Matsumura, M., and Bondarenko, P. V. (2008) Isomerization of a single aspartyl residue of anti-epidermal growth factor receptor immunoglobulin gamma 2 antibody highlights the role avidity plays in antibody activity. *Biochemistry 47*, 2518−2530.
(11) Demeule, B., Shire, S. J., and Liu, J. (2009) A therapeutic antibody and its antigen form different complexes in serum than in phosphate-buffered saline: a study by analytical ultracentrifugation. *Anal. Biochem. 388*, 279−287.
(12) Philo, J. S. (2001) Overview of the quantitation of protein interactions. *Curr. Protoc. Protein Sci.*, Suppl. 17, Chapter 20.
(13) Oda, M., Uchiyama, S., Robinson, C. V., Fukui, K., Kobayashi, Y., and Azuma, T. (2006) Regional and segmental flexibility of antibodies in interaction with antigens of different size. *FEBS J. 273*, 1476−1487.
(14) Tito, M. A., Miller, J., Walker, N., Griffin, K. F., Williamson, E. D., Despeyroux-Hill, D., Titball, R. W., and Robinson, C. V. (2001) Probing molecular interactions in intact antibody: antigen complexes, an electrospray time-of-flight mass spectrometry approach. *Biophys. J. 81*, 3503−3509.
(15) Schuck, P. (2000) Size-distribution analysis of macromolecules by sedimentation velocity ultracentrifugation and Lamm equation modeling. *Biophys. J.*, 1606−1619.
(16) Wen, J., Arakawa, T., and Philo, J. S. (1996) Size-exclusion chromatography with on-line light-scattering, absorbance, and refractive index detectors for studying proteins and their interactions. *Anal. Biochem. 240*, 155−166.
(17) Gabrielson, J. P., Randolph, T. W., Kendrick, B. S., and Stoner, M. R. (2007) Sedimentation velocity analytical ultracentrifugation and SEDFIT/c(s): limits of quantitation for a monoclonal antibody system. *Anal. Biochem. 361*, 24−30.
(18) Bekker, P. J., Holloway, D. L., Rasmussen, A. S., Murphy, R., Martin, S. W., Leese, P. T., Holmes, G. B., Dunstan, C. R., and DePaoli, A. M. (2004) A single-dose placebo-controlled study of AMG 162, a fully human monoclonal antibody to RANKL, in post-menopausal women. *J. Bone Miner. Res. 19*, 1059−1066.
(19) Fenn, J. B., Mann, M., Meng, C. K., Wong, S. F., and Whitehouse, C. M. (1989) Electrospray ionization for mass spectrometry of large biomolecules. *Science 246*, 64−71.
(20) Paternoster, L., Lorentzon, M., Vandenput, L., Karlsson, M. K., Ljunggren, O., Kindmark, A., Mellstrom, D., Kemp, J. P., Jarett, C. E., Holly, J. M., Sayers, A., St, P. B., Timpson, N. J., Deloukas, P., Davey, S. G., Ring, S. M., Evans, D. M., Tobias, J. H., and Ohlsson, C. (2010) Genome-wide association meta-analysis of cortical bone mineral density unravels allelic heterogeneity at the RANKL locus and potential pleiotropic effects on bone. *PLoS Genet. 6*, 1−12.
(21) Nabipour, I., Larijani, B., Vahdat, K., Assadi, M., Jafari, S. M., Ahmadi, E., Movahed, A., Moradhaseli, F., Sanjdideh, Z., Obeidi, N., and Amiri, Z. (2009) Relationships among serum receptor of nuclear factor-kappaB ligand, osteoprotegerin, high-sensitivity C-reactive protein, and bone mineral density in postmenopausal women: osteoimmunity versus osteoinflammatory. *Menopause 16*, 950−955.
(22) Bowsher, R. R., and Sailstad, J. M. (2008) Insights in the application of research-grade diagnostic kits for biomarker assessments in support of clinical drug development: bioanalysis of circulating concentrations of soluble receptor activator of nuclear factor kappaB ligand. *J. Pharm. Biomed. Anal. 48*, 1282−1289.
(23) Ferrant, J. L., Wilson, C. A., Benjamin, C. D., Hess, D. M., Hsu, Y. M., Karpusas, M., Roux, K. H., and Taylor, F. R. (2002) Variation in the ordered structure of complexes between CD154 and anti-CD154 monoclonal antibodies. *Mol. Immunol. 39*, 77−84.